

Realization of a Conductive Bridging RF Switch Integrated onto Printed Circuit Board

Etienne Perret^{1, 2, *}, Thais Vidal¹, Arnaud Vena³, and Patrice Gonon⁴

Abstract—This paper presents a new approach for the realization of RF switches based on the Conductive Bridging Random Access Memory technology (CBRAM). This promising approach allows the realization of RF switches in an extremely simple manner at low cost. For the first time, an RF switch based on a MIM structure is realized with an insulator layer obtained from a commonly used resin deposited by spin coating. The paper reports a RF switch based on CBRAM and demonstrates a device integration onto plastic circuit board (PCB). The realized switch is validated by experimental measurements for a frequency range up to 1.5 GHz with an activation voltage less than 1 V.

1. INTRODUCTION

With the tremendous development in means of communication in recent decades, the importance of wireless communications has increased considerably, leading designers to new challenges such as the development of versatile systems. To connect people to each other and across the Internet, RF designers need to invent new multi-band and broadband RF circuits, particularly for telephony. Thus, RF switches will play a key role not only in wireless communications, but also in sensors and actuators of tomorrow. RF switches are basic components that allow reconfiguration of devices when they operate in order to make them more agile. They are present in all communication systems and allow for instance signals multiplexing, so as to reconfigure or dynamically control the system. The performances of such devices can even impact the choice of the hardware architecture to be implemented in order to achieve the desired functionality. This is why a broadband solution, based on a flexible and low cost approach, where the power consumption of the switch is reduced, is eagerly awaited. Today's technological solutions (solid state and radiofrequency microelectromechanical (RF MEMS) based systems) need some improvements to meet the challenges of the future. For examples, MEMS rest on heavy manufacturing technologies, requiring an important number of masks. Even if RF MEMS fabricated using printed circuit processing techniques has been proposed [1], most of the time, such components are expensive and associated with an extremely rigid manufacturing process. The same complexity is observed in the design phase, where mechanical and thermal considerations also have to be taken into account.

Current efforts focus on the future generations of memories [2–4]. The stakes are high, and the development of new non-volatile memories, is expected to revolutionize the architectures of future computer systems. Many emerging technologies are contending for supremacy, phase change (PC) memory and resistance (switching) random access memory (ReRAM) among them. The common point between these two technologies is that both have been evaluated for implementation in RF switches. The specific dielectric used in PC materials can switch between amorphous (high resistance) phase and crystalline (low resistance) phase upon application of thermic energy that can be in the form

Received 4 December 2014, Accepted 5 February 2015, Scheduled 11 March 2015

* Corresponding author: Etienne Perret (etienne.perret@LCIS.grenoble-inp.fr).

¹ University Grenoble Alpes, LCIS, 50, rue de Laffemas, BP 54, Valence 26902, France. ² Institut Universitaire de France, 103 Boulevard St-Michel, Paris 75005, France. ³ Institut d'Electronique du Sud, Place Eugène Bataillon, Montpellier 34095, France.

⁴ LTM CNRS, CEA, Grenoble 38000, France.

of voltage and current [3]. High performance RF switches based on PC materials have been recently obtained [5, 6]. But the fabrication process remains complex and costly. Classical microfabrication clean-room technology, high temperature processes, very specific dielectrics or even Joule heating simulations are required. On the other hand, ReRAM which exhibits electrically switchable resistance, has also attracted considerable attention in recent years [2]. Among these families of resistive memory cells, the CBRAM technology rests on the electrochemical dissolution properties of an active electrode: the metallic ions thus generated move through the solid electrolyte in order to form a conductive metal bridge joining the other electrode, which is inert. The commutation of the device is thus obtained [7]. CBRAM are recognized by the International Technology Roadmap for Semiconductors (IRST) [8] as sufficiently mature and powerful to be considered as very good candidates for the realization of future memories. Based on this technology, which comes from microelectronics, it has been shown that the operating principle of these memories can be used to realize RF switches. A new family of RF switches using this principle and called Conductive Bridging RF Switch (CBRFS) recently appeared [9–11]. The feasibility of a RF switch operating between 1 to 6 GHz has been demonstrated [9, 10]. In this frequency band, the switch has comparable performances to those that are currently obtained with traditional approaches such as MEMS or solid state switches [10]. The CBRAM technology has shown the potential to operate at lower energies and voltage (couple of volts), making it particularly interesting for embedded applications. As compared to MEMS, CBRFS has lower switching time, dimensions and cost. In [11], a multilayer structure based on CBRAM and realized without any photolithography process has been proposed. This approach is simpler to implement, and therefore, potentially compatible with printed electronic techniques. Moreover, integrating RF switches on a printed circuit board (PCB) — which is also a very challenging task — seems possible with such approaches. In both cases, the compatibility should be maintained with standard printed electronic and PCB manufacturing technologies. For technological reasons, it is easier to stack different layers together (even for layers of hundreds of nanometers) than to realize tens of micron gaps between electrodes made with different metals. Unlike [9, 10] wherein a chalcogenide glass doped with silver ions is used, in [11], the solid electrolyte is simply a SiO_2 layer deposited by evaporation.

In order to be even closer to a completely printed RF switches solution, we describe a novel RF switch made with a polymer resin, a common material that can be easily deposited by spin coating. No complex technological, high temperature process such as photolithography or doping is used. Instead, the approach is simple to implement and compatible with direct integration of the RF switches in conventional RF PCB. The study that follows aims to demonstrate the implementation of these MIM structures on a low cost and versatile substrate, massively used in the electronics manufacturing process for signal switching applications.

2. CONCEPT OF THE RF SWITCH BASED ON CBRAM

2.1. Operating Principle

CBRFS are based on MIM solid state structures (Metal Insulator Metal), i.e., a stack of three layers with no moving parts, as shown in Figure 1(a). By carefully choosing materials and their thicknesses, it is possible to show that such a structure acts as a programmable resistor that keeps its value in the absence of energy to maintain its state. This stack must be composed of an inert electrode (Al, Ni...)

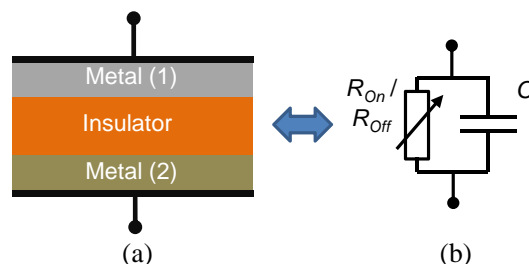


Figure 1. CBRAM Cell: (a) MIM structure, (b) electrical equivalent circuit.

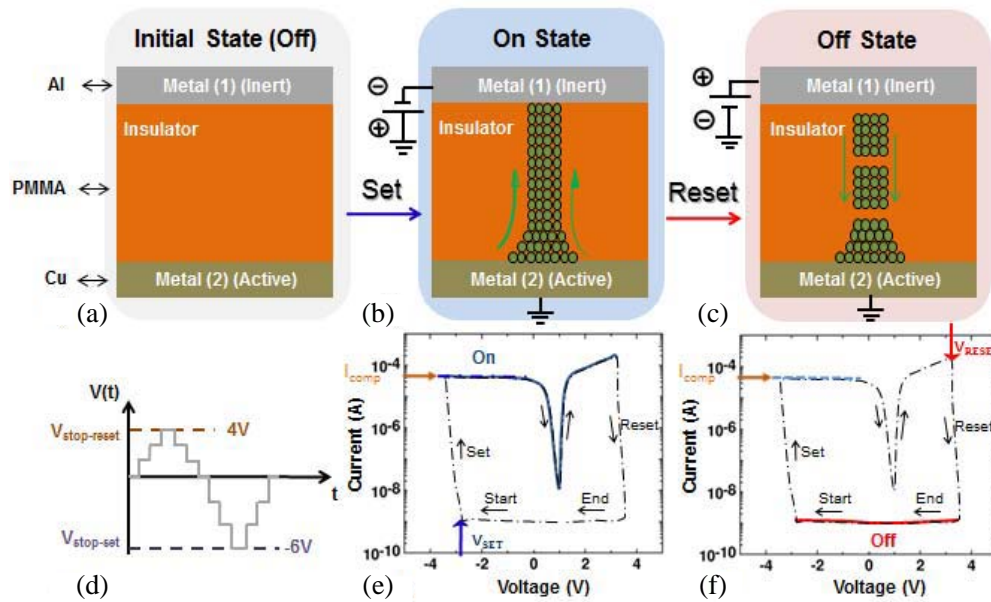


Figure 2. Operating principle of the CBRAM cell. (a) Initial Off state. (b) Transition to the On state. (c) Return to the Off state. The polarization of the cell is indicated on the drawings. (d) Variation of the bias voltage as a function of time, the typical tension variation value used here is 1 V/s. (e) Typical changes in current/voltage across a CBRAM cell, transition to the On state (SET). (f) Transition to the Off state (RESET).

and the other must be chemically active (Cu, Ag...). An equivalent electric diagram of the structure is shown in Figure 1(b). It comprises a variable resistance (relating to the On and Off states) in parallel with a capacitor, which depends on the geometry of the MIM structure and the nature of the dielectric layer. Initially, the structure is not conductive (denoted Off state in Figure 2(a)) because the electrolyte is a good insulator. Under the action of a tension V_{set} between the two electrodes, the insulator allows the migration of Cu ions, which come from the active electrode, towards the inert electrode (see Figure 2(b) [12]). The ions are then deposited on the inert electrode and are reduced with electrons to obtain the Cu metal. Thus, a conductive filament grows until it touches the active electrode. As we can see in Figure 2(e), the device then switches to a conducting (On) state (SET). To break the filament and return to the Off state (RESET), we have to simply reverse the voltage (see Figure 2(f)). The nature of the dielectric plays an important role in the establishment of the conductive bridge. The most widely used ones are chalcogenides [7], polymer [13] and oxides [14]. In this study, Poly(methyl methacrylate) (PMMA) is used. This commonly used resin mixed with a solvent to form a liquid can be simply deposited by spin coating. After a short curing (about 100°C during 1 min, which is the highest temperature reached during the fabrication process.) we obtain a solid thin layer with few hundred nanometers of thickness. Moreover, this resin has the advantage of being printable [15], which makes this RF switches' technology potentially compatible with standard printed electronics manufacturing process.

2.2. CBRAM Approach for RF Applications

Currently, CBRAM are mainly designed to produce the next generation of non-volatile memories [8]. The objective here is to reuse their operating principle for the realization of RF switches. The expected specifications are very different from those memories and require a specific work using RF skills.

For memory applications, consumption, switching and memory access time are critical. In RF, it is the frequency behavior, in particular, the ratio between the On and Off state, which is decisive. More precisely, the figure of merit of a switch is linked to the product of the On state resistance (R_{On}) by the capacitance C . This product has to be minimized to obtain better performances. Given the

specificities of each application, one of the main differences between memories and the RF switches is regarding the dimensions of the structures. Indeed, in RF, the miniaturization of the cell is not critical; the switch must be sized to have a specific frequency behavior. It is thus necessary to ensure a capacitor value C as low as possible on the largest frequency range. Thus, a configuration with a thick dielectric layer (as compared to the classical thicknesses used for memory) appears as one of the most promising candidates, thanks to the possibility of decreasing the RF capacitor between the two electrodes.

3. EXPERIMENTAL VALIDATION AND PRACTICAL ISSUES

Initial MIM structures were made like the one presented in [11], a simple stacking of three layers made of different materials, without taking the RF accesses into consideration. These structures were used to validate the switching nature of the component and to characterize some important values, such as threshold voltages (V_{set} and V_{reset}) that have to be used to set and reset the switch. We used a conventional RF substrate (Rogers RO4003C), which acts as a board, but also provides the first metal electrode of the MIM structure, namely, the active electrode of copper (Cu) with a thickness of 17 microns. Then, a PMMA dielectric layer of 90 nm was obtained using the spin coating process. Finally, the aluminum (Al) electrodes were deposited by evaporation (100 nm thickness), using a metal mask with a large number of circular holes. One of the structures produced is shown in Figure 3(a). I–V characterizations were performed with a programmable sourcemeter (Keithley 2635A) connected to a probing station. The PMMA layer was removed from a corner of the sample to connect a tungsten tip to the Cu bottom electrode. The second probe, a gold wire, was placed on the upper Al electrode. Thus, while imposing a bias voltage, the current and the voltage were measured over time at the terminals of the structure. Each programming cycle was composed of a positive triangle signal followed by a negative triangle signal (see Figure 2(d)). Meanwhile, we imposed a limitation current, which could be set unequally between the positive and negative sections of the cycle.

The first ten programming cycles (set/reset) of the CBRAM cell are shown in Figure 4. The switching behavior observed was also confirmed for other pads, and at each time several re-programming cycles were possible. This shows that the desired switch function is compatible with the use of common materials, such as standard RF substrates, PMMA as insulator and aluminum as inert electrode. As expected, during the initial cycles, we observe that the SET voltages (V_{set} equal to -3 V – 5 V) and the RESET voltages (V_{reset} equal to 2 V) are higher than for the other cycles. The programming current used is always limited to 1 mA . After the process of bridge forming, the SET voltage stabilizes at around -0.5 V and the voltage RESET around 1 V . The values of the On and Off state resistors, extracted from

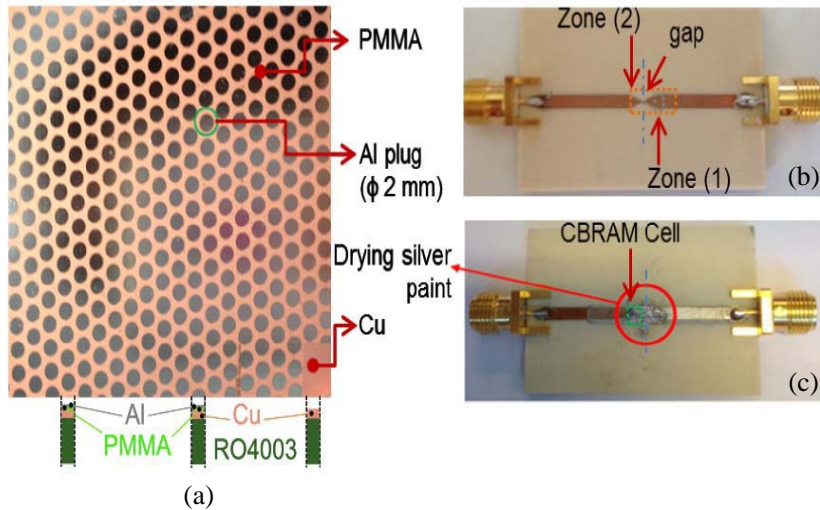


Figure 3. (a) Picture of the Cu/PMMA/Al CBRAM cell, description of the different layers. (b) $50\ \Omega$ microstrip line. (c) $50\ \Omega$ microstrip line with the CBRFS at the center.

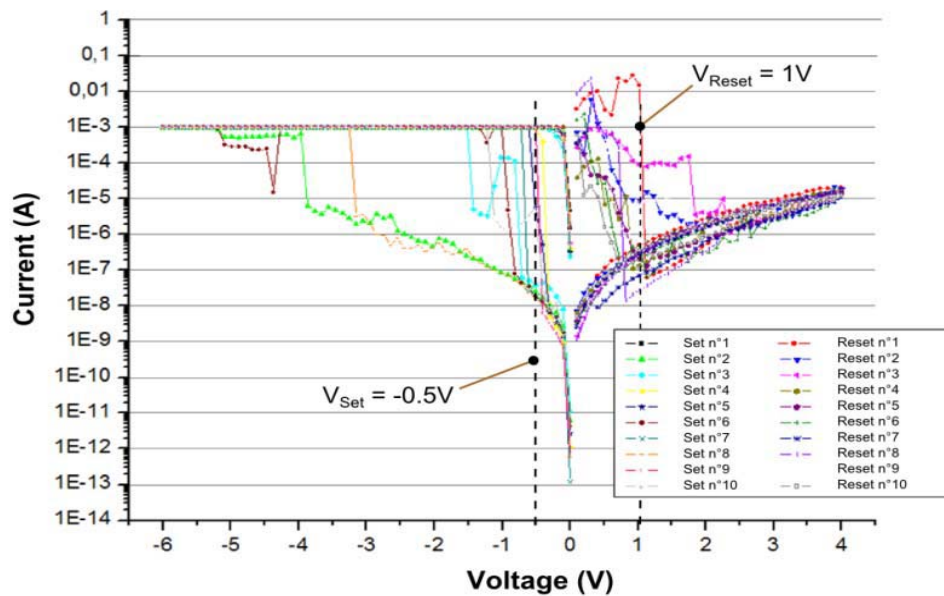


Figure 4. Measured set/reset programming cycle of the Cu/PMMA/Al CBRAM cell. The PMMA thickness is 90 nm. The programming current is limited to 1 mA.

the results are $R_{On} = 50 \Omega$ and $R_{Off} = 10 \text{ M}\Omega$. As expected, activation voltages are much lower than those found in [11], where for a SiO_2 layer of 160 nm, a threshold voltage switching was found to be 7 V. These values are of the same order of magnitude as those of [9, 10] ($V_{set} = -1 \text{ V}$ and $V_{reset} = 1 \text{ V}$), where a dielectric doped with Ag ions was used. We observe that the switch can operate more than ten programming cycles (set/reset). However, after a few tens of cycles the component is blocked on keep one of the two states. This behavior is sensitive to the manufacturing process; the results can be highly variable from one plot to another. We believe that a specific work dedicated to the technology process is expected to increase the switch life.

To validate the implementation of the CBRAM cell on a RF circuit, a 50Ω characteristic impedance microstrip line has been used as shown in Figure 3(b), where a switch has been performed at the center of the line (see Figure 3(c)). The CBRAM cell, i.e., the Cu/PMMA/Al stack of layers, has been made by manually using a Kapton masking tape. PMMA has been deposited on the entire surface of the sample, with the exception of a small area situated at one end of the microstrip line near the gap region, i.e., the zone (1) described in Figure 3(b). At the end of the process, this area allows connecting the aluminum electrode to the part of the copper line that will not include the CBRAM cell. The Kapton tape is removed and then a new area is masked using Kapton: the entire sample is covered, except for a small area situated at the center of the line (see the zone (2) in Figure 3 (b)). This area corresponds to the precise location of the MIM structure (see Figure 3(c)) plus the connection between the upper electrode and the second part of the microstrip line. To end the manufacturing process, a layer of aluminum 100 nm thick is deposited by evaporation. We observe that the voltage to activate the switch can be applied directly between the two parts of the microstrip line by using the inner conductor of the SMA connectors.

Three different structures were realized, but only one was operational. This is likely due to the non-uniformity of PMMA deposit caused by the copper layer roughness. For measuring S parameters, this structure was connected to a VNA. A voltage generator was connected to the rear panel of the VNA in order to add the DC component to the RF signal. In this way, a difference of potential was applied between the inner conductors of the two coaxial lines of the VNA, that is, between the two metal electrodes of the CBRAM cell. Despite the presence of a sufficient voltage to SET the switch, no changes in the S parameters were observed. The structure kept the same behavior as a shorted line, i.e., the structure in Figure 3(b): the RF line without the CBRAM cell. This behavior is caused by the thickness of the weak aluminum electrodes. This effect could be easily eliminated by increasing Al

thickness. But as it was not possible to use the previously employed evaporation system to increase the thickness of the inert electrode significantly, we chose to manually deposit a layer of silver filled epoxy resin on the zone (2), as shown in Figure 3(c). As described in Figure 2(b), to set the switch, a negative voltage is applied between the two electrodes. The measurement results obtained are shown in Figure 5, where one can see the variations in frequency of the S -parameters for different negative values of the voltage applied between two of the access lines. From 0 V to $|-2\text{ V}|$, the switch is in an On state. An insertion loss (S_{21}) of less than 4 dB is obtained up to 2.5 GHz. When the absolute value of the voltage is increased, the switch gradually commutes from the On state to the Off state. This transition is clearly observable in Figure 5. Thus, for voltage values above $|2\text{ V}|$, the switch is in an Off state with an insertion loss (S_{21}) less than -10 dB over the entire band 0–1.5 GHz. Thereafter, positive voltages were applied to the switch; the results are shown in Figure 6.

Observations are quite similar to the one obtained with positive voltages: for low positive values (below 1.5 V), the switch goes back to an On state; for higher voltages, it returns to the Off state.

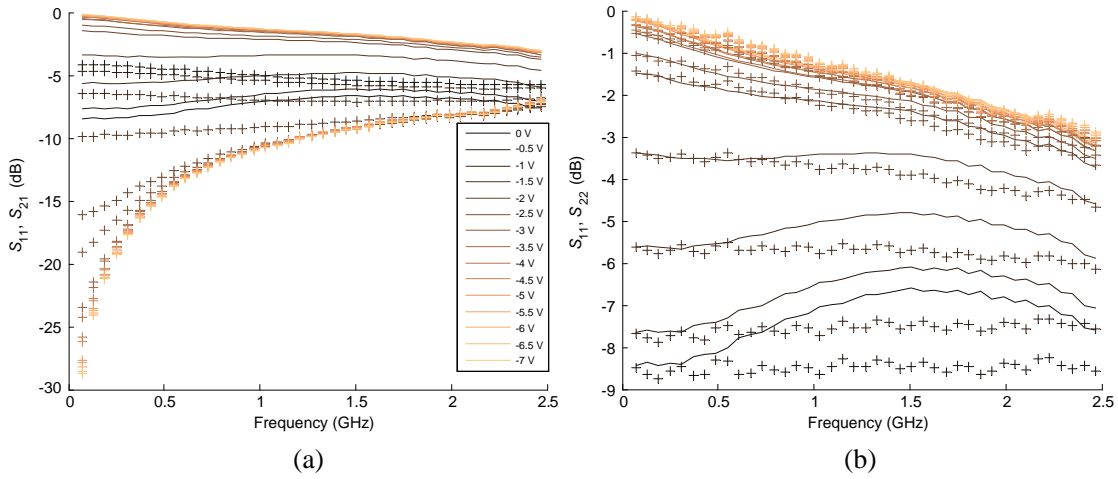


Figure 5. S parameters measured for the CBRFS (Figure 3(c)) with respect to the tension (negative variations) of polarization. (a) (—) The return loss (S_{11}), (+++) the insertion loss (S_{21}). (b) (—) The return loss (S_{11}), (+++) the return loss (S_{22}).

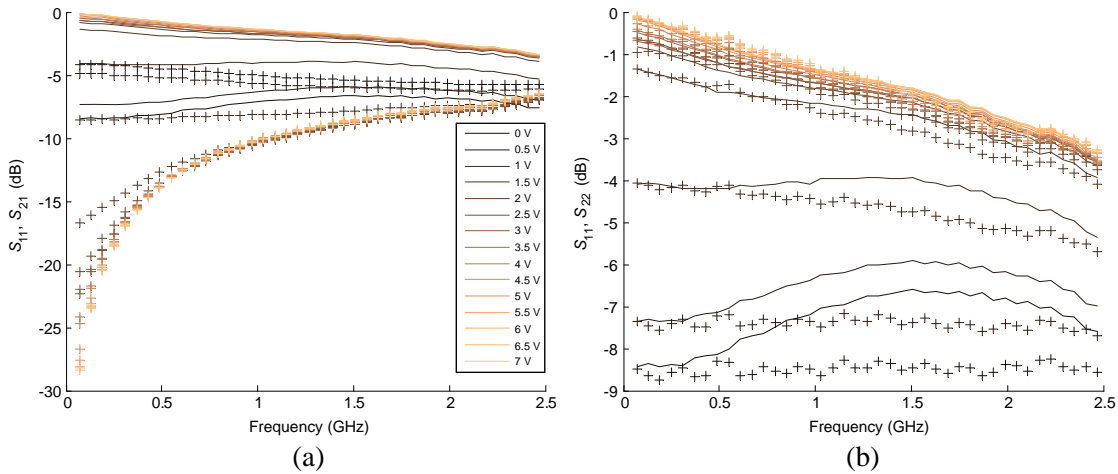


Figure 6. S parameters measured for the CBRFS (Figure 3(c)) with respect to the tension (positive variations) of polarization. (a) (—) The return loss (S_{11}), (+++) the insertion loss (S_{21}). (b) (—) The return loss (S_{11}), (+++) the return loss (S_{22}).

Table 1. Positioning of the CBRFS presenting here in relation to others' work. Comparison of principal properties.

	Present work	[11]	[10]	[6]
Frequency Range	DC to 1.5 GHz	DC to 0.15 GHz	DC to 6 GHz	DC to 20 GHz
Insertion Loss	4 dB	1.6 dB	0.5 dB	2.5 dB
Isolation	10 dB	20 dB	35 dB	15 dB
Actuation Voltage	1 V–2 V	7 V	1 V	1 V
Fabrication process	Simple/Common material	clean room	clean room	clean room

The observed behavior is clearly different from that of the MIM Cu/PMMA/Al structure previously characterized with the DC probing system. This behavior can be explained by the presence of the silver layer, which has been added to the aluminum electrode. Indeed, silver is known to be an active electrode, and it has even smaller activation energy than copper for diffusion in dielectric substrate. This means that silver ions can diffuse into the structure to create a filament when a positive voltage is applied. The presence of the two active electrodes gives a symmetric behavior to the switch; in this case, the Set and Reset voltages are similar with a value of around zero Volt [2, 3, 16]. Positioning of the CBRFS presented here in relation to others' work is done in Table 1. It is clear that the device reported in this manuscript did not demonstrate improved performance in comparison to others works [6, 10]. However, the realization process is totally different, common materials are used and a clean room is not required.

4. CONCLUSION

In this paper, we described the implementation of CBRFS with a technique commonly used in the electronics manufacturing process. The approach has a great potential to be compatible with printed electronics techniques. An RF switch having two distinct states over a frequency range of 0–1.5 GHz was obtained from a conventional stack made of three materials, particularly by using a PMMA resin as the insulator layer. No complex deposition or photolithography process has been used. This shows the versatility and the huge potential of such an approach. Indeed, our approach is based on a simpler manufacturing technique (fewer manufacturing steps, which do not require the use of etching processes, based on common materials. . .) and could be compatible in the future with low cost printing techniques conducted using a dielectric ink, or with common printed circuit techniques. In the latter case, RF circuits including RF switches could be realized simultaneously by a classical PCB manufacturer. The results are encouraging and can be used to solve the problem of CBRAM integration on to PCB. The proposed technique is very promising for the realization of RF switches, but the reliability of these devices is still weak and needs further work for improvement. Indeed there is still a lot of room for improvement of the CBRFS performances. CBRFS should have a significant impact in the future thanks to its simple structure, low cost, non-volatility and low voltage activation, and should successfully compete with current solutions that require much more complex processes for their realization.

ACKNOWLEDGMENT

The authors wish to thank the Up-line Technological Platform (PTA) for their technical support.

REFERENCES

1. Silva, M. W. B., S. E. Barbin, and L. C. Kretly, "Fabrication and testing of RF-MEMS switches using PCB techniques," *2009 SBMO/IEEE MTT-S International Microwave and Optoelectronics Conference (IMOC)*, 96–100, 2009.
2. Valov, I., R. Waser, J. R. Jameson, and M. N. Kozicki, "Electrochemical metallization memories — Fundamentals, applications, prospects," *Nanotechnology*, Vol. 22, 254003, 2011.

3. Derhacopian, N., S. C. Hollmer, N. Gilbert, and M. N. Kozicki, "Power and energy perspectives of nonvolatile memory technologies," *Proceedings of the IEEE*, Vol. 98, 283–298, 2010.
4. Huang, G. M. and Y. Ho, "Memristors for non-volatile memory and other applications," *Advances in Non-Volatile Memory and Storage Technology*, Y. Nishi, Ed., Woodhead Publishing, 2014.
5. Shim, Y., G. Hummel, and M. Rais-Zadeh, "RF switches using phase change materials," *2013 IEEE 26th International Conference on Micro Electro Mechanical Systems (MEMS)*, 237–240, 2013.
6. Crunteanu, A., A. Mennai, C. Guines, D. Passerieux, and P. Blondy, "Out-of-plane and inline RF switches based on $\text{Ge}_2\text{Sb}_2\text{Te}_5$ phase-change material," *IEEE MTT-S International Microwave Symposium (IMS)*, 1–4, Tampa Bay, Florida, US, 2014.
7. Kund, M., G. Beitel, C. U. Pinnow, T. Rohr, J. Schumann, R. Symanczyk, K. D. Ufert, and G. Muller, "Conductive bridging RAM (CBRAM): An emerging non-volatile memory technology scalable to sub 20 nm," *IEEE International Electron Devices Meeting, IEDM Technical Digest*, 754–757, 2005.
8. "The international technology roadmap for semiconductors (ITRS)," 2011, Available: <http://www.itrs.net/>.
9. Nessel, J. A., R. Q. Lee, C. H. Mueller, M. N. Kozicki, M. Ren, and J. Morse, "A novel nanoionics-based switch for microwave applications," *2008 IEEE MTT-S International Microwave Symposium Digest*, 1051–1054, 2008.
10. Nessel, J. and R. Lee, "Chalcogenide nanoionic-based radio frequency switch," Patent No. US8410469 B2, USA, 2013.
11. Vena, A., E. Perret, S. Tedjini, C. Vallée, P. Gonon, and C. Mannequin, "A fully passive RF switch based on nanometric conductive bridge," *IEEE MTT-S International Microwave Symposium (IMS)*, 1–3, Montreal, Canada, 2012.
12. Russo, U., D. Kamalanathan, D. Ielmini, A. L. Lacaita, and M. N. Kozicki, "Study of multilevel programming in programmable metallization cell (PMC) memory," *IEEE Transactions on Electron Devices*, Vol. 56, 1040–1047, 2009.
13. Potember, R., T. Poehler, and D. Cowan, "Electrical switching and memory phenomena in CuTCNQ thin films," *Applied Physics Letters*, Vol. 34, 405–407, 1979.
14. Bernard, Y., V. Renard, P. Gonon, and V. Jousseume, "Back-end-of-line compatible conductive bridging RAM based on Cu and SiO_2 ," *Microelectronic Engineering*, Vol. 88, No. 5, 814–816, 2011.
15. De Gans, B.-J., L. Xue, U. S. Agarwal, and U. S. Schubert, "Ink-jet printing of linear and star polymers," *Macromolecular Rapid Communications*, Vol. 26, 310–314, 2005.
16. Vianello, E., C. Cagli, G. Molas, E. Souchier, P. Blaise, C. Carabasse, G. Rodriguez, V. Jousseume, B. De Salvo, F. Longnos, F. Dahmani, P. Verrier, D. Bretegnier, and J. Liebault, "On the impact of Ag doping on performance and reliability of GeS_2 -based conductive bridge memories," *2012 Proceedings of the European Solid-State Device Research Conference (ESSDERC)*, 278–281, 2012.